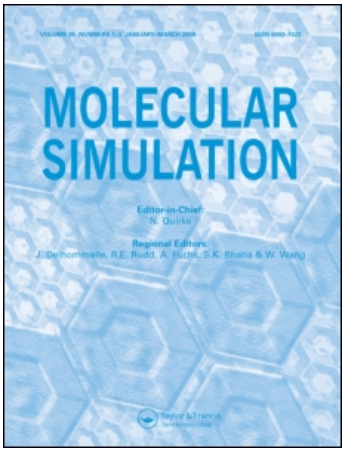

Molecular Simulation
Publication details, including instructions for authors and subscription information:
http://www.informaworld.com/smpp/title~content=t713644482

Molecular dynamics simulation of helium-argon gas mixture under various wall conditions

Ilyas Kandemir[a]; Fatih Erdogan Sevilgen[b]
[a] Department of Design and Manufacturing Engineering, Gebze Institute of Technology, Kocaeli, Turkey [b] Department of Computer Engineering, Gebze Institute of Technology, Kocaeli, Turkey

To cite this Article Kandemir, Ilyas and Sevilgen, Fatih Erdogan(2008) 'Molecular dynamics simulation of helium-argon gas mixture under various wall conditions', Molecular Simulation, 34: 8, 795 — 808
To link to this Article: DOI: 10.1080/08927020802275785
URL: http://dx.doi.org/10.1080/08927020802275785

Molecular Simulation
Vol. 34, No. 8, July 2008, 795–808

Taylor & Francis
Taylor & Francis Group

Molecular dynamics simulation of helium–argon gas mixture under various wall conditions

Ilyas Kandemir[a]* and Fatih Erdogan Sevilgen[b1]

[a]*Department of Design and Manufacturing Engineering, Gebze Institute of Technology, Kocaeli, Turkey;* [b]*Department of Computer Engineering, Gebze Institute of Technology, Kocaeli, Turkey*

(*Received 5 April 2008; final version received 15 June 2008*)

As computational capabilities increase, molecular dynamics (MD) simulations become important tools of simulating reality. These simulations are especially useful for compressible gas mixture problems. In this study, binary diffusion of helium and argon was examined using a hard-sphere MD simulation method. For the sake of computational speed, low spacing ratios were chosen. Binary mass diffusion of gases in two equally sized halves of a box was simulated for identical initial kinetic energies and number densities. It has been noted that a purely mass diffusion mechanism of different gases is not physically possible. The resultant gas mixtures of several diffusion simulations were used as initial conditions for combined heat transfer – Couette flow, and heating and cooling experiments. The results showed the interesting behaviour of the mixture, which was subjected to various wall conditions. Energy of heavier molecules is found to be more sensitive to the wall velocities and less sensitive to the wall temperatures than lighter molecules. Diffusion, heat transfer, viscosity and heat capacity coefficients are deduced as well.

Keywords: molecular dynamics; simulation; helium–argon; binary mixture; hard-sphere

1. Introduction

Molecular simulation approaches to gas dynamics problems have recently gained popularity as computational capabilities have increased. Among these studies, hard-sphere calculations are used in order to achieve high number of molecules and low Knudsen number (Kn) simulations with less computational expense. As Knudsen number decreases, continuum model becomes valid ($Kn < 0.01$). Molecular dynamics (MD) simulations also provide more accurate analyses for higher Knudsen numbers offering clues for continuum.

The most important parameters prescribing the behaviour of a gas system are transport coefficients. By estimating the variation of these coefficients, heat transfer, momentum transfer and mass diffusion phenomena can be examined. Assessment of these parameters is especially difficult for gas mixtures. MD methods can be utilised in estimation of these parameters.

In this study, the behaviours of gas mixtures in simple binary diffusion, Couette flow, simple heat transfer, cooling and heating are examined by using a multi-cell hard-sphere MD simulation method. Along with these basic simulations, coupled effects of heat transfer and Couette flow are also examined. Based on these simulations, transport coefficients are deduced and helium–argon selected as the binary gas mixture. These two gases have very different molecular masses (mass ratio 1/10) and different molecular sizes (diameter ratio 1/1.67). Therefore, it is possible to examine, in the simulations mentioned above, the effects of molecular size and mass on gas behaviour.

Although the quantitative results of this study can hardly be used in most practical applications, the qualitative results observed may be very helpful in understanding the behaviour of a gas mixture. In order to run low Kn simulations, one prefers to deal with low mean free paths and consequently low spacing ratios. Knudsen numbers used in the simulations of this study were as low as 0.03 while the spacing ratio was five within the computational domain of a box.

2. Background

Kinetic theory considers a gas as a collection of particles [1,2]. The equation introduced by Maxwell and Boltzmann is regarded as the foundation of kinetic theory constituting the microscopic mathematical model of a gas [3–5]. Chapman and Enskog's solution to this equation reveals the general transport terms in the transport phenomena [6–8]. Rahman investigates a liquid by considering the Lennard-Jones potential of continuously interacting particles in [9].

With the advances in computer capabilities, microscopic simulations on kinetic theory have become possible and several simulation techniques have been developed. Direct Simulation Monte-Carlo (DSMC) method is a popular randomised technique used in studies based on molecular collisions, derived from the kinetic theory, on several areas such as micro-channel flows and rarefied gas dynamics [10]. However, by its deterministic nature, MD

*Corresponding author. Email: kandemir@gyte.edu.tr

ISSN 0892-7022 print/ISSN 1029-0435 online

DOI: 10.1080/08927020802275785
http://www.informaworld.com

simulations yield more accurate and realistic results especially in representing transport phenomena, heat capacities and compressibility. Since MD requires the calculation of all molecular interactions, it necessitates quite high computational resources [11,12]. Methods, such as multi-cell, have been developed to decrease the CPU demand of MD closer to the order of that of DSMC. On a single processor, Knudsen number of less than 0.01 was achieved in a hard-sphere single specie non-equilibrium gas simulation by MD [13]. Currently, on a single machine, a number of hundreds of millions of molecules is considered to be achievable for short MD simulations. On the other hand, a DSMC study involving 7 billion molecules was carried out using more than 32,000 processors in parallel [14].

Several features of noble gases were examined in previous gas mixture studies focused on various aspects [15–17]. Especially in the analysis of transport phenomena, if possible, taking advantage of MD simulations was advised by many researchers [18,19]. For different cases, transport coefficients were calculated using MD in many studies as well [20–22].

3. Computational model

In this study, the computational region is a rectangular parallelepiped domain (box). Intermolecular collisions are elastic, yielding a hard sphere MD model. Post-collision velocities of a colliding pair are calculated based on the molecular masses, diameters, pre-collision velocities and positions of the colliding particles. The algorithm for the calculation of post-collision velocities is developed simply by satisfying the momentum and energy equations, keeping the elastic behaviour in mind.

For the sake of computational speed, a multi-cell method described by Kandemir [13] was used. The method considers the computational region as a union of sub regions called cells. As the possibility of the collision of distant particles is low, collision events between molecules in the same cell or neighbour cells are sought. Molecules are allowed to cross the cell boundaries and their neighbour cells change in the course of cell-crossing events. Since molecules can undergo collisions after several cell-crossing events, none of the real collisions is actually lost. The outer boundaries of the box coincide with the boundaries of the outermost cells; a molecule reaching to this boundary generates a special kind of cellular event called wall collision. In this method, a time variable is associated with each molecule, eliminating the need of repositioning of all molecules after each event. This approach not only greatly reduces the incremental errors incorporated by the positional updates, but also affects the computational speed positively.

This study involves the examination of binary diffusion process along with the behaviour of the resultant gas mixture under some predefined effects. In order to simulate a binary diffusion, the box was initially considered as if it was separated by a specular wall of zero thickness. The monatomic gas particles (balls) of each molecular kind were located in one-half of the box. As the initial conditions of the adjustment period, the centres of particles are spaced equally, and the molecular kinetic energies of all particles are set to be the same. This resulted in the same uniform number density and temperature profiles in both halves, providing the opportunity of generating (after adjustment period) good initial conditions for mass diffusion and minimising the effects of diffusion of other kinds (Figure 1). The initial direction of every molecule, on the other hand, is randomly selected, so that a good Maxwellian distribution may develop after a few collisions per particle in each half. Non-dimensional properties that specify the molecular species under examination were chosen as in Table 1.

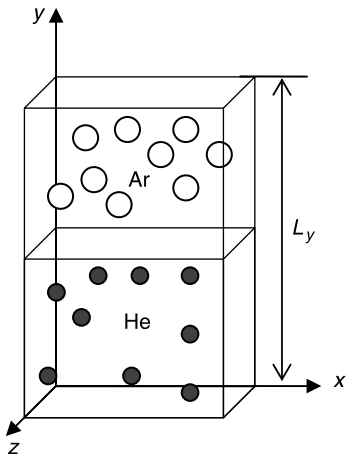

Figure 1. Computational domain of the simulation showing unmixed monatomic gases.

The event-driven process of the whole simulation is carried out by finding and processing the next event in the computational domain. Data reductions and long time averaging were performed after every real collision. All six outer walls and both sides of the separating wall in the middle were considered specular; balls bounce off the wall elastically during the initial adjustment phase. After the adjustment phase and observing the Maxwellian

Table 1. Non-dimensional molecular properties of gases in this study.

Gas	Mass	Diameter	Initial speed
Helium	1	1	$\sqrt{10}$
Argon	10	1.67	1

behaviour, the separating wall was removed which starts the diffusion. When the diffusion was over and the uniform density profiles settled, the simulation was stopped. The resulting gas mixture, involving each molecule's positional, velocity and time information, was used as the initial condition in the runs we performed, afterwards.

The MD simulation of gas mixtures was aimed to explore the behaviour of certain physical characteristics of predetermined numerical transport experiments. In these runs, complete periodicity condition was used on the $\pm x$ and $\pm z$ outer limits of the box. According to this condition, any molecule that leaves the computational domain through a wall is introduced at the opposite wall with the same velocity and relative position. That is to say that periodicity condition decreases the molecule's x_i position by $\pm L_i$ when it reaches $a \pm x_i$ outer limit, where L_i is the size of the box in x_i direction and the subscript i is either 1 (for x) or 3 (for z). In this implementation of periodicity, the molecule can collide with other molecules around both opposite walls.

The wall condition in $\pm y$ directions was selected as a modified diffuse reemission condition. For example, a diffusely reemitted helium molecule's position and time is unchanged after a wall collision. However, regardless of impingement velocity and direction, its velocity components are randomly selected as if it was coming from an equilibrium gas of helium behind the wall with a given gas temperature equals to the specified wall temperature. The input parameters required by diffuse wall calculation were incoming molecular kind, wall temperature and wall velocity (needed in Couette flow simulations).

In this study, MD simulations were conducted for helium–argon gas mixture using various upper/lower wall temperature and wall velocity combinations: simple conduction, simple Couette flow (identical fixed wall temperatures), Couette flow with symmetric wall temperatures and cooling and heating of the domain through the upper and lower walls with fixed temperatures.

4. Simulation results

4.1 Binary diffusion

In binary diffusion simulations, hard spheres representing helium and argon molecules were located in separate halves of the computational domain; lower and upper halves were filled with helium and argon molecules, respectively. Initially, the same number of molecules were positioned equally spaced in each domain. Each particle initially had equal molecular energy while directions of the velocities were randomly selected. Then the simulation was started and molecules were allowed to adjust to the regional properties.

4.1.1 Speed distributions

Upper and lower walls of the box were specular during this initial adjustment period. The specular wall separating the two halves caused the speed distributions evolved towards the Maxwellian distribution separately. Although, the average molecular energies for two kinds were identical, since helium and argon have different molecular masses, their average speeds were not the same.

In Figure 2, the speed distributions corresponding to the unmixed gases are presented based on a snapshot data after 10 cpp (collision per particle). In this plot, values are normalised considering the molecular masses in order to compare the results with the normalised speed distribution.

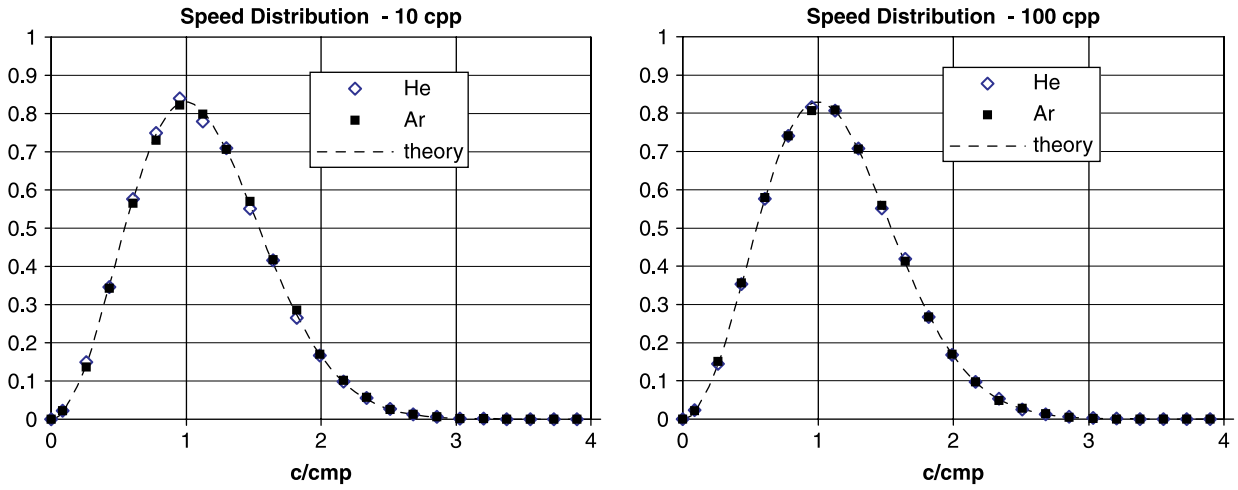

Figure 2. Comparison of normalised speed distribution of steady unmixed (after 10 cpp) and steady mixed (after 100 cpp) He and Ar with the theory. $N = 110{,}592$; $N_{He} = N/2$; $N_{Ar} = N/2$; $s/d_{He} = 5$ and $Kn \cong 0.269$.

c being speed and the index mp denoting the most probable value, the results show perfect agreement with the theoretical normalised distribution function

$$F(\xi) = \frac{4}{\sqrt{\pi}} \xi^2 e^{-\xi^2}, \quad (1)$$

where $\xi = c/c_{mp}$.

After the initial adjustment period, the separating specular wall was taken out and diffusion started. The unsteady behaviour of diffusion continued until a good uniform gas mixture was formed. After the steady state conditions were well established (100 cpp), another snapshot of speed distribution was generated and this is presented in Figure 2. The graphs in Figure 2 are quite similar, suggesting that the speed distributions for each kind in the hard-sphere binary gas mixture are consistent with the theory.

4.1.2 Behaviour of diffusion

Since the temperature and number density in each half are equal, the mixing process may be expected to be a pure mass diffusion. However, as explained below, the expected behaviour was not observed (Figure 3). The apses in Figure 3 correspond to the y-axis of the computational domain. The leftmost column shows the time elapsed during the diffusion process in terms of collisions per particle (cpp) and time unit.

In this particular simulation, L_y (the box size in the direction of diffusion) was selected smaller compared to the other two dimensions ($L_y/L_x = L_y/L_z = 1/8$), in order to create a faster diffusion. Because of the high number of molecules, we are still able to collect enough data for clear plots. It is also worth mentioning that the sharp decays at the walls are due to the higher molecular size of argon molecules and their inability to position very close to the walls. Note that, molecular positions are represented by the locations of their centres. The region of data reduction was chosen according to the all possible positions of helium molecules. Therefore, a sub-region of size ($d_{Ar} - d_{He} = 0.67$) near the walls cannot be occupied by argon molecules, causing sharp local decreases in the profiles. Similarly, sharp density decays near the middle wall are caused by this absence of molecules in that region.

It has been noted that the smaller and lighter helium molecules diffuse into the heavier argon gas faster than the argon diffuse into helium. Argon's number density profile after six collisions per particle shows a net density increase at the opposite half. This is due to the large mass ratio between the two molecular kinds. It was also observed that the system converges into a steady gas mixture in about 10 cpp.

When we have a closer look at the energy distributions, we notice that right after the removal of the middle wall, an energy wave is generated in the middle and penetrates into the halves. As time passes, this wave becomes stronger and at 4 cpp, the energy at the helium's half is higher than the argon's side. One may expect an energy increase at the argon's half because of the higher diffusion of faster helium molecules and the amount of convective energy they carry with. However, although argon molecules do not penetrate into the other half as fast as helium molecules do, they transfer their energy to the helium causing an energy increase in helium's region. The binary (He–Ar) collision rate profile at 1 cpp and later shows this energy transfer mechanism.

Examination of graphics on number of collision in Figure 3 yields that molecules tend to make collisions with molecules of other kind. This feature was considered being dominated by the homogenous characteristics of the mixture. Smaller molecules simply fill the spaces among the bigger ones. Of course, the evolution of this collision frequency is expected to depend upon overall number density and molecular sizes.

By comparing columns 1 and 3 in Figure 3, one can easily verify that the number of binary (He–Ar) collisions profiles bears a resemblance to the variations of total number density. Not surprisingly, the same connection was observed among self-collision (He–He or Ar–Ar) and number density profiles of related species.

4.2 Combined heat conduction and Couette flow

4.2.1 Profiles of flow properties

Couette flow simulations were accomplished simply by imposing upper and lower wall conditions. Fully mixed gas obtained from the diffusion simulations was used for each velocity and temperature difference (DT–V_x). Wall velocity and temperature differences affect the diffusely reemitted molecules' velocity components on y-wall collisions. This effect traverses through the fluid and profiles of flow characteristics develop.

For various combinations of upper and lower wall temperature and velocity differences, u_x (local average velocity x-component), n (number density), T and E (energy) profiles along the y dimension within the computational domain are examined. In these experiments, total number of molecules is $N = 38{,}400$ with equal number of molecules for each kind ($N_{He} = N_{Ar} = N/2$), box size is $L_x \times L_y \times L_z = 100 \times 480 \times 100$, centre-to-centre molecular spacing is $s = 5.0$, and molecular sizes are $d_{He} = 1$ and $d_{Ar} = 1.67$. Initial average speed for Ar molecules is $\sqrt{3/2}$ (which corresponds to $c_{mp} = 1$). Four different wall velocity pairs are examined: $\pm V_x = 0.3, 0.6, 0.9$ and 1.2. Knudsen number deduced from the simulations is approximately $Kn \cong 0.033$.

Long time average results for pure wall-velocity driven Couette flow runs are presented in Figure 4, based on the normalisations described above. In these runs, wall

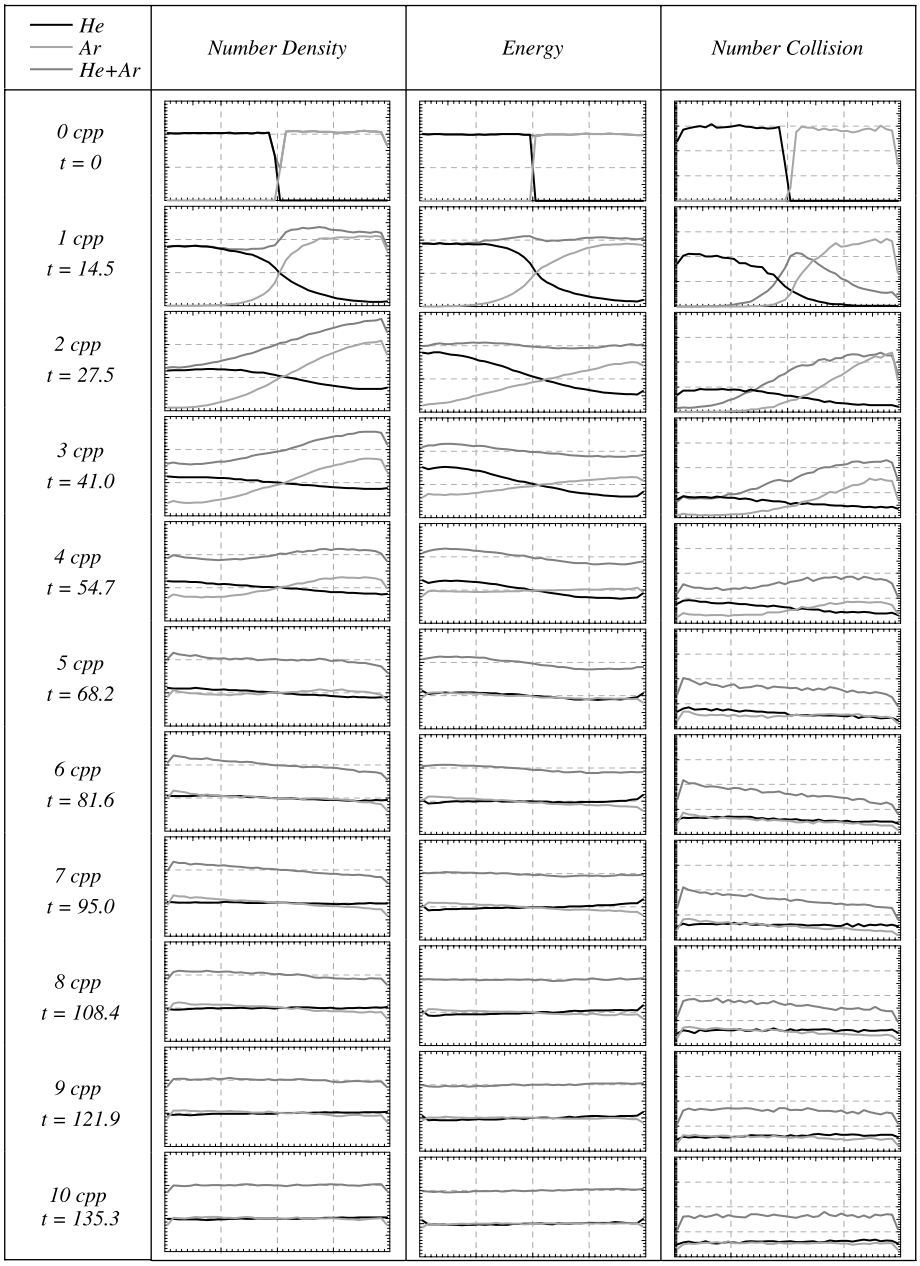

Figure 3. Evolution of number density, energy and collision distribution in He–Ar binary diffusion.

temperatures are same, which are approximately equal to the average global temperature in the fixed wall case (that is denoted by black filled circles). Upper and lower walls are moved with the same but opposite velocities resulting in simple Couette flow simulations.

Temperature values in Figures 4(g)–(i) are deduced from the dimensional definition

$$3kT \equiv \langle m|\vec{c} - \vec{u}|^2\rangle = \sum_{i=1}^{\sigma} \frac{n_i}{n} m_i \langle|\vec{c}_i - \vec{u}|^2\rangle, \qquad (2)$$

where k is Boltzmann's constant, T is temperature, $\vec{u}$ is local velocity vector, index i represents the molecular kind, n_i represents number of molecules of kind i in the local region of occupancy, n is total number of molecules in that particular region, σ is number of molecular kinds, and $\langle\,\rangle$ represents an averaging operator over the sampling range. Note that

$$n_1 + n_2 + \cdots + n_\sigma = n \qquad (3)$$

and for our problem $\langle c_{x_i}\rangle = |\vec{u}| = u_x$ as only x component of velocity vector is significant in simple Couette flow.

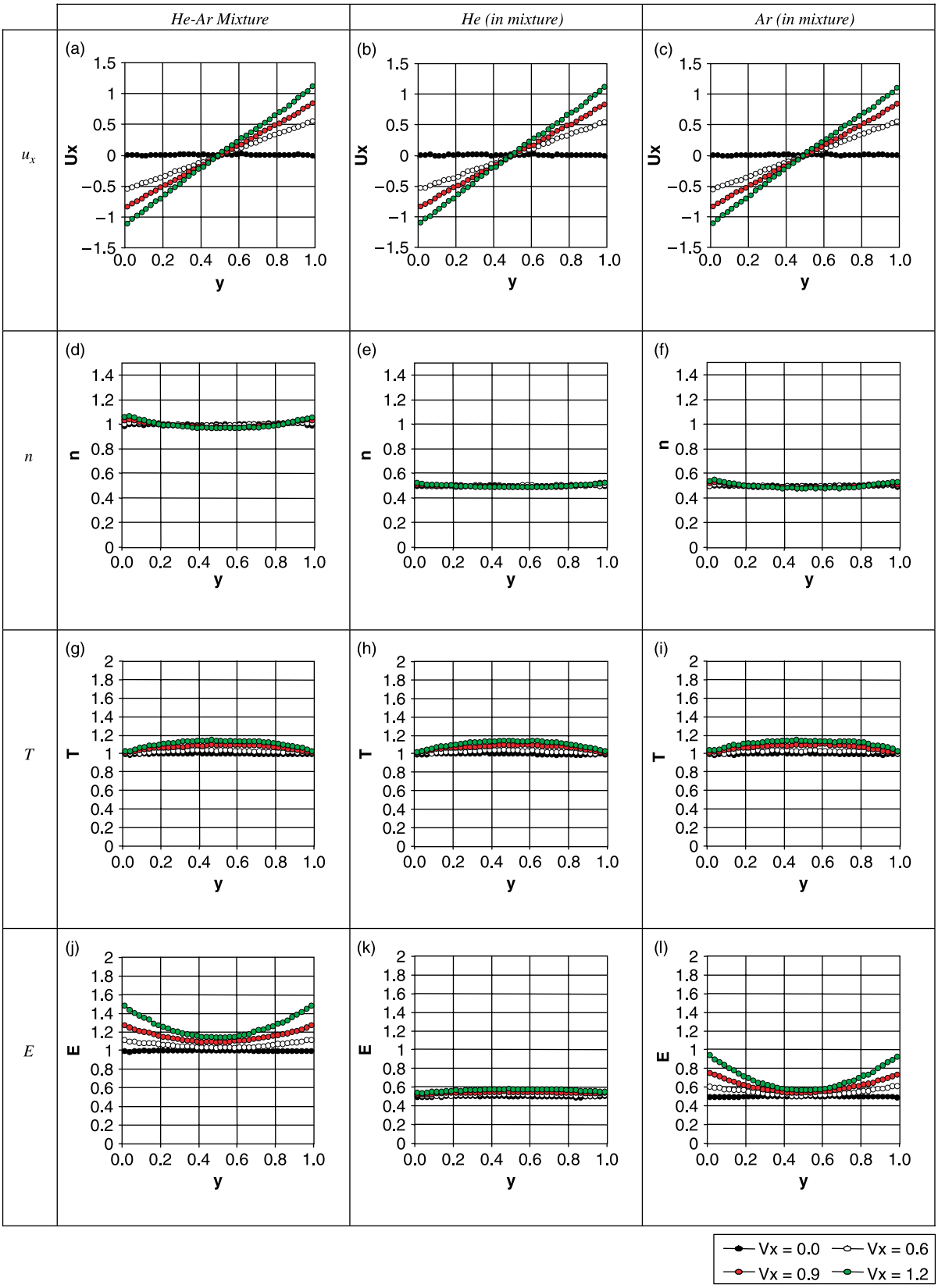

Figure 4. Velocity (u_x, (a)–(c)), number densiy (n, (d)–(f)), temperature (T, (g)–(i)), and energy (E, (j)–(l)) profiles in Couette flow for the mixture, He only, and Ar only in the He–Ar mixture. N = 38400 DT = 0.0 s/dHe = 5 Kn ≅ 0.033.

Therefore, one can easily verify that

$$\langle|\vec{c}_i - \vec{u}|^2\rangle = \langle c_i^2\rangle + u_x^2 - 2u_x\langle c_{x_i}\rangle = \langle c_i^2\rangle - u_x^2. \quad (4)$$

It is observed that velocity and temperature profiles for He and Ar in Figures 4(b) and (c) and Figures 4(h) and (i), respectively, are alike. Therefore, the mixture behaves the same way (Figures 4(a) and (g)). Kinetic energy profiles on the other hand show remarkable difference simply because moving walls impart higher energy on heavier particles, where the molecular energy is defined as

$$E \equiv \frac{1}{2}mc^2. \quad (5)$$

Figure 4(k) suggests that, although average molecular energy for He molecules slightly increases as V_x gets bigger, the linearity of the profile hardly changes. Energy of argon molecules however, is highly affected by the wall velocities, as shown in Figure 4(l), presenting radical increases near the walls. This energy increase is due to the higher magnitudes of x-velocity components of argon molecules near the walls. Since temperature is not simply equal to the average local kinetic energy when there is a flow, this x-velocity component increase does not necessarily raise the temperature near the walls, as seen in Figures 4(g) and (i).

It is worth mentioning that the linearity of the u_x profiles is due to the low Knudsen number ($Kn \to 0$) [22]. The analytical solution of conservation laws for Simple Couette flow, for μ/κ being constant (which is a very common case in a large application range), suggests that the temperature in the middle is

$$T_m = T_w + \frac{\mu}{\kappa}\frac{V_x^2}{2}, \quad (6)$$

where μ is dynamic viscosity and κ is heat transfer coefficient of the fluid in the domain. Note that the temperature profiles qualitatively agrees with this result even though there is no assumption of any kind directly associated with the ratio of transport coefficients in MD simulations. Using the transport coefficients deduced later in this study, quantitative agreement of these profiles with the above theoretical formulation was observed, as well.

Number density profiles in Figures 4(d)–(f) show the effect of temperature increases away from the walls (Figures 4(g)–(i)) with corresponding density drops. The small density drops on the walls in Figures 4(d) and (f) are due to the non-existence of centres of larger argon molecules in those regions. Here, Figure 4(a) is simply the superposition of Figures 4(b) and (c), just like in Figures 4(j)–(l). He and Ar molecular kinds roughly behave similarly on number density profiles. A closer look on Figures 4(e) and (f) yields that although different molecular kinds in a mixture follow the identical temperature profiles, their density profiles may not be the same in simple Couette flow of gas mixtures.

Using Equations (2)–(5)

$$3kT = 2\langle E\rangle - \langle m\rangle u_x^2 \quad (7)$$

can be found, which is completely in good agreement with the qualitative behaviour of velocity, energy and temperature profiles in Figure 4.

The difference in profiles of kinetic energy seen in simple Couette flow of gas mixtures for different species affects the speed distributions, which are normalised with the same manner in Figure 2. Therefore, even though speed distributions for low wall velocity values resemble normalised speed distribution of steady mixed He and Ar in Figure 2, high V_x distributions show radical differences, as seen in Figure 5. The distributions for species in Figure 5 are normalised based on the same theoretical value (not per their actual most probable value) in order to show the difference in the distributions for the different kinds. Correspondingly, Figure 5 agrees with the Figures 4(k) and (l).

Long time average results for pure heat conduction runs are presented in Figure 6. In these runs, upper and lower walls are fixed. Temperature on the walls, on the other hand, is deviated from the average ($T_0 = 1$) by $\pm$DT = 0.0, 0.1, 0.2 and 0.3. As seen in Figures 6(d)–(f) temperatures of species and mixture match the temperatures on the walls satisfying the imposed boundary conditions. Again, the almost-linearity of these profiles stems from the low Knudsen number.

Figures 6(d) and (g) are identical, simply because there is no significant local velocity ($u_x = 0$), unlike in Couette flow, and therefore temperature is proportional to the energy, satisfying the Equation (7). Comparison of Figures 6(h) and (i) yields that when there is no apparent

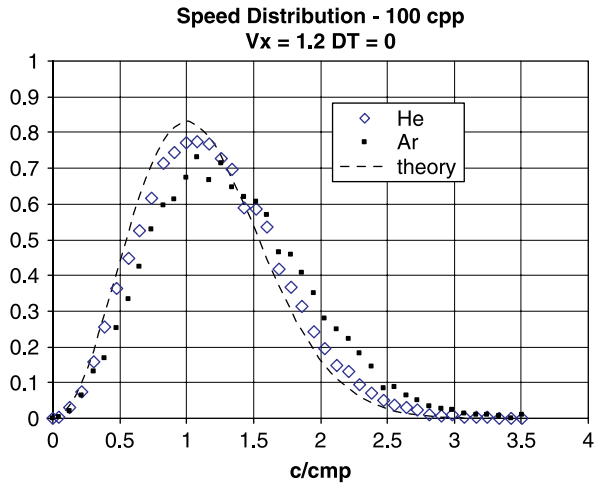

Figure 5. Normalised speed distribution of steady mixed He and Ar in simple Couette flow. $N = 38{,}400$; $N_{He} = N/2$; $N_{Ar} = N/2$; $s/d_{He} = 5$ and $Kn \cong 0.033$.

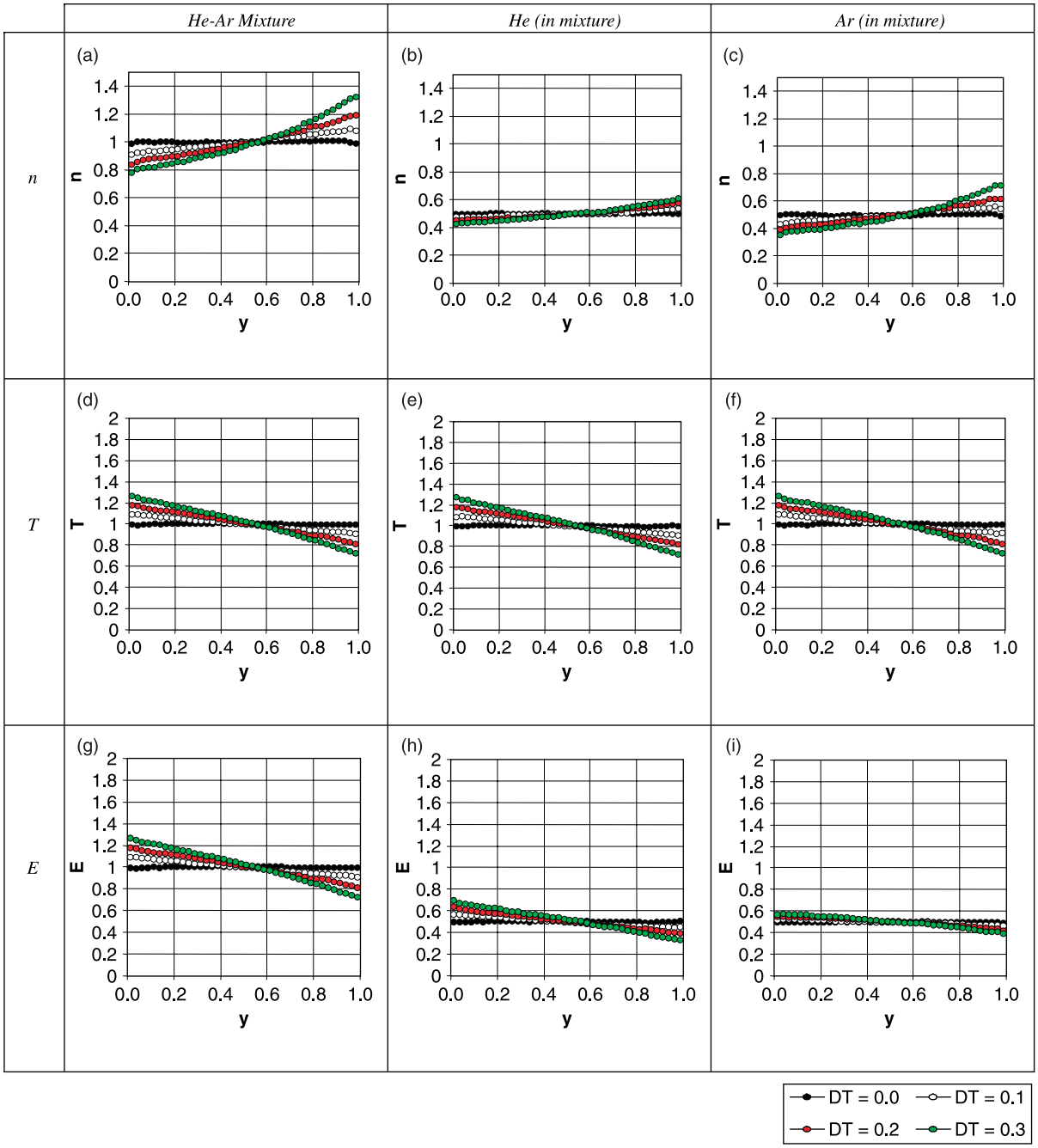

Figure 6. Number density (n, (a)–(c)), temperature (T, (d)–(f)), and energy (E, (g)–(i)) profiles in heat conduction for the mixture, He only, and Ar only in He–Ar mixture. N = 38400; $s/d_{He} = 5$; Kn ≅ 0.033.

heat conduction (DT = 0), energy in the computational domain is equally partitioned among the different species. When we apply temperature difference on the walls, however, energy of helium molecules is affected more than that of argon molecules. In simple Couette flow, on the other hand, energy of helium molecules is almost unaffected by the imposed wall velocities. As in Figures 4 and 6, number density and energy profiles of mixture are given as the superposition of the profiles of the species on the right two columns.

Normalised temperature profiles of different molecular kinds in Figures 6(e) and (f) are alike. Since kinetic energy profiles of helium are steeper, this can only be achieved if corresponding number density profiles of helium are less affected by the temperature gradient compared to those of argon (Equation (2)). Examination of Figures 6(b) and (c)

confirms this condition. Therefore, partial temperature profiles of the species are the same with the heat conduction, just like in simple Couette flow.

While linear temperature profiles occur, the non-linearity of number density profiles in Figure 6(a) makes it possible to have a negligible pressure gradient for the mixture, as it is expected, complying with the state equation

$$p = nkT, \tag{8}$$

where p represents the static pressure.

In order to examine the coupled effect of heat and velocity differences on the walls, simulations with various DT–V_x pairs were carried out. The profiles deduced from these simulations are presented in Figure 7.

Figures 7(a)–(c) suggest that velocity condition is the major factor in the formation of velocity profiles. Therefore, Figures 7(a)–(c) and 4(a)–(c) are alike, showing no significant outcome stemming from the heat conduction. This resembles the uncoupled solution of momentum and energy equations in solving velocity for an incompressible case. However, the simulations did not impose such restrictions on the fluid. As a result, velocity profiles in coupled simulations should differ anyhow. Indeed, a closer look in Figures 7(a)–(c) yields that the profiles are not symmetrical, and $u_x = 0$ takes place somewhere closer to the cold wall.

Based on the comparison of Figures 7(d)–(f) with Figures 6(a)–(c), one can easily see that the existence of wall velocities ($V_x \neq 0$) shifts the average number density points (y at $n = 1$) in the related profiles towards the cold wall. Note that, the shifts are more obvious in temperature (Figures 7(g)–(i)) and energy (Figures 7(j)–(l)) profiles.

Once again, normalised velocity and temperature profiles of species and mixtures are consecutively alike in Figure 7. As a result, one may conclude that partial velocity values of molecular kinds in a mixture behave similarly, just like the temperature.

In Figures 6(h) and (i), temperature gradient caused less effect on argon's energy profiles whereas in Figures 4(k) and (l) velocity gradient highly affected them. If both hold in coupled simulations, energy profiles of argon gas in Figure 7(l) should show same large energy increase near the walls along with less asymmetry compared to helium's profiles in Figure 7(k). In fact, this behaviour is exactly observed in the figures mentioned, with corresponding density formations.

As a result, while velocity gradient affects the energy profiles of heavier argon molecules, temperature gradient has effects mostly on the lighter helium molecules' energy profiles, and correspondingly on argon's number density profiles.

Simulations with different numbers of molecules, DT–V_x combinations, and aspect ratios of computational domain were conducted. As main behaviours presented here were observed in those, they were not illustrated in this study for the sake of reduction.

4.2.2 Transport coefficients

Heat conduction and viscosity coefficients deduced from the He–Ar gas mixture simulations were compared with the theoretical values. Results were compared with previous studies.

As considered as a mono-component gas, for each monatomic molecular kind used in the mixture, kinetic theory viscosity coefficient from Enskog's result may be written as

$$\mu_{\mathrm{KT}} = \frac{\sqrt{mkT_0}}{\pi^{3/2} d^2}, \tag{9}$$

and taking Prandtl number, $Pr = 2/3$ for the monatomic gas and specific heat ratio $\gamma = C_{\mathrm{p}}/C_{\mathrm{v}} = 5/3$, conductivity coefficient may relate to viscosity coefficient as [13]

$$\kappa_{\mathrm{KT}} = \frac{15}{4}\frac{k}{m}\mu_{\mathrm{KT}}. \tag{10}$$

Therefore, determination of viscosity coefficient is sufficient for the estimation of heat conduction coefficient in this kinetic theory approach.

In order to formulate the transport coefficients of the mixture, the following approximations are used. Viscosity coefficient is

$$\mu_{\mathrm{mix}} = \sum_{i=1}^{\sigma} \frac{n_i \mu_i}{\xi_i}, \tag{11}$$

where

$$\xi_i = \sum_{j=1}^{\sigma} n_j \phi_{ij}, \tag{12}$$

and inter-collisional parameter according to Wilke's approximation is

$$\phi_{ij} = \frac{\left(1 + \sqrt{\frac{\mu_i}{\mu_j}}\sqrt[4]{\frac{m_j}{m_i}}\right)^2}{\sqrt{8\left(1 + \frac{m_i}{m_j}\right)}}. \tag{13}$$

Correspondingly, for thermal conductivity, Wassiljewa's equation is

$$\kappa_{\mathrm{mix}} = \sum_{i=1}^{\sigma} \frac{n_i \kappa_i}{\psi_i}, \tag{14}$$

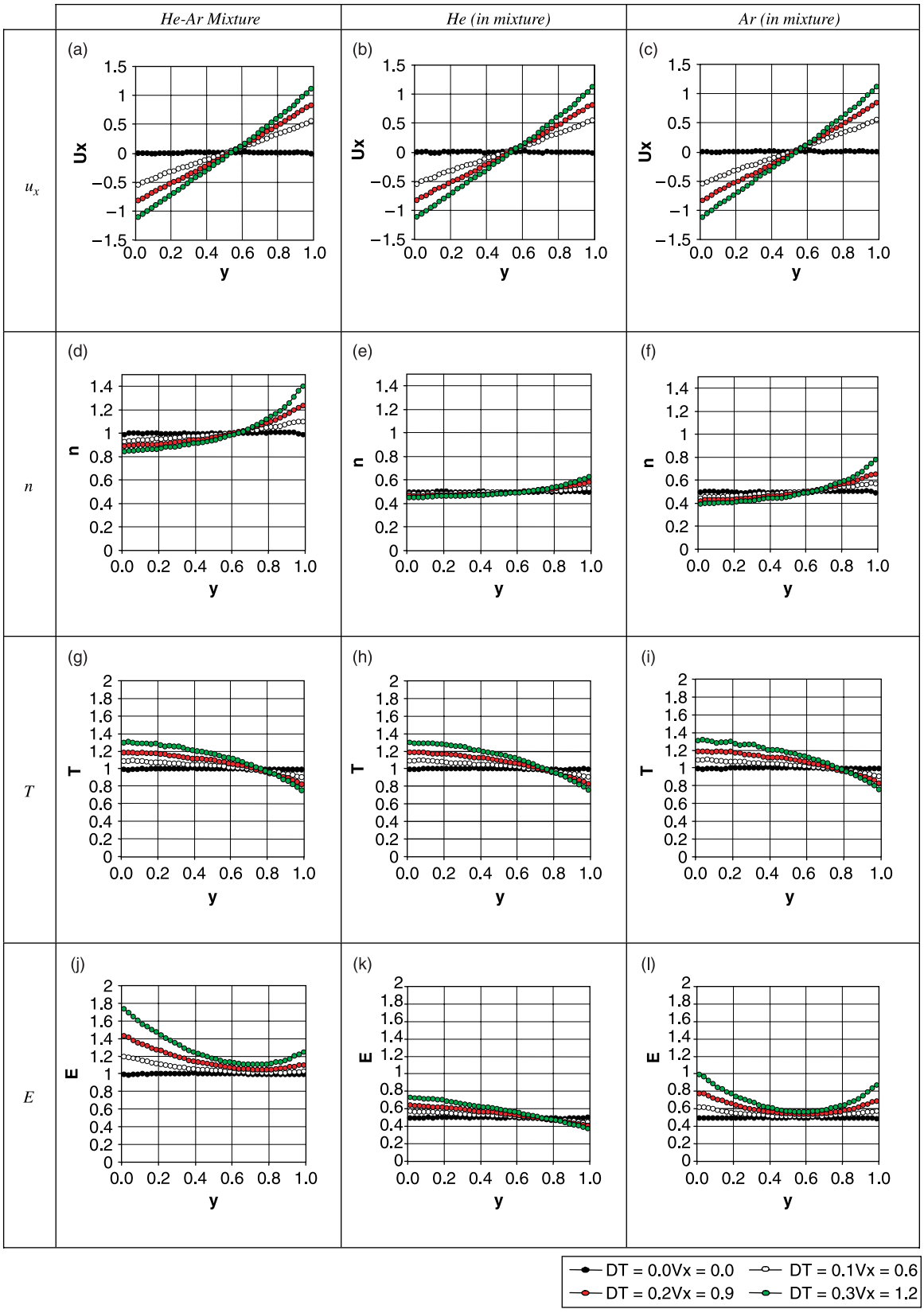

Figure 7. Velocity (u_x, (a)–(c)), number density (n, (d)–(f)), temperature (T, (g)–(i)), and energy (E, (j)–(l)) profiles in coupled effects for the mixture, He only, and Ar only in He–Ar mixture. N = 38400; $s/d_{He} = 5$; Kn ≅ 0.033.

where

$$\psi_i = \sum_{j=1}^{\sigma} n_j A_{ij}, \tag{15}$$

and Lindsay–Bromley correlation may be simplified, for Sutherland constants being neglected compared to the temperature, as [23]

$$A_{ij} \cong \frac{\left(1 + \sqrt{\frac{\mu_i}{\mu_j}}\left(\frac{m_j}{m_i}\right)^{3/8}\right)^2}{4}. \tag{16}$$

Note that, $\phi_{11} = \phi_{22} = 1$ and $A_{11} = A_{22} = 1$ for a binary mixture.

Theoretically, mean free path of the mixture in a local region can be calculated using the formula [24]

$$\lambda_{\text{th}} = \sum_{i=1}^{\sigma} \left(\frac{n_i}{n} \left[\sum_{j=1}^{\sigma} \left\{ \pi d_{ij}^2 n_j \sqrt{1 + \frac{m_i}{m_j}} \right\} \right]^{-1} \right), \tag{17}$$

where

$$d_{ij} = \frac{d_i + d_j}{2}. \tag{18}$$

Again theoretically, Knudsen number in any simulation is

$$Kn_{\text{th}} = \frac{\lambda_{\text{th}}}{L_y}. \tag{19}$$

Conductivity coefficient was deduced from the simulations by processing the total kinetic energy of the incoming and outgoing molecules on a y-wall in δt time interval, using the following relationship:

$$\kappa_{\text{sim}} = \frac{L_y}{2(\text{DT})} \frac{1}{L_x L_z} \frac{1}{\delta t} \frac{1}{2} \sum \left[\left(mu^2\right)_{\text{in}} - \left(mu^2\right)_{\text{out}} \right]_{\text{wall}}. \tag{20}$$

Similarly, x-momentum of incoming and outgoing molecules on the wall is accumulated for the estimation of viscosity coefficient in a Couette flow simulation:

$$\mu_{\text{sim}} = \frac{L_y}{2(V_x)} \frac{1}{L_x L_z} \frac{1}{\delta t} \sum \left[(mu_x)_{\text{in}} - (mu_x)_{\text{out}} \right]_{\text{wall}}. \tag{21}$$

Based on these definitions and approaches, for different combinations of wall velocities and temperatures and for different total numbers of molecules, the deduced transport coefficients with corresponding Knudsen numbers and simulation mean free path values are tabulated in Table 2.

It was noted in Table 2 that the mean free path values deduced from the heat transfer simulations are lower than those from simple Couette flow runs. For no temperature difference and zero velocity gradient runs (DT = 0 and $V_x = 0$), the mean free path values are almost identical. It was also noted that mean free path values deduced from the pure heat conduction runs are lower than those from simple Couette flow runs. As Knudsen number increases, it was observed that the mean free path values from simple Couette flow runs slightly decrease. An opposite behaviour was observed in simple conduction runs. At this point, it is worth mentioning that the aspect ratio in the runs of the lowest Knudsen number in the table is different from those of others.

The transport coefficient ratios in Table 2 are found to be decreasing as *Kn* increases. This behaviour was observed in previous theoretical studies and single species MD simulations [22,25]. The variations of the heat conduction and viscosity coefficients presented in the table not only qualitatively comply with the unmixed gas results, but also quantitatively approach to them. Especially the variation of viscosity coefficient almost perfectly fit in the previous single-component results. Note that, the calculated transport coefficients are for low Knudsen number He–Ar gas mixture and their calculation did require neither Sutherland constants nor critical temperature values. This may suggest that, such simple

Table 2. Transport properties in the MD simulations of He–Ar gas mixture at different low Knudsen numbers.

N	DT	V_x	L_y	L_x, L_z	λ_{sim}	$\kappa_{\text{sim}}/\kappa_{\text{mix}}$	$\mu_{\text{sim}}/\mu_{\text{mix}}$	Kn_{th}
38,400	0	0	480	100	15.889			0.0337
38,400	0.3	0	480	100	15.753	0.794		0.0337
38,400	0	1.2	480	100	16.510		0.948	0.0337
16,384	0	0	320	80	15.892			0.0505
16,384	0.3	0	320	80	15.765	0.747		0.0505
16,384	0	1.2	320	80	16.475		0.935	0.0505
6912	0	0	240	60	15.884			0.0673
6912	0.3	0	240	60	15.833	0.715		0.0673
6912	0	1.2	240	60	16.454		0.907	0.0673

$s_{\text{He}} = 5$; $\lambda_{\text{th}} = 16.155$; $N_{\text{He}} = N/2$ and $N_{\text{Ar}} = N/2$.

MD simulations may be used in the estimation of the transport coefficients of gas mixtures.

4.3 Heating and cooling

Heating and cooling of the mixture and the response of the gas were also examined. Results were compared with the theoretical expectations.

Cooling and heating of the He–Ar gas mixture were carried out like the heat transfer runs were with the exception of that both (upper and lower) walls were kept at the same fixed temperature. If this fixed wall temperature is lower or higher than the average temperature of the pre-mixed gas, it works as a cooling or heating effect on the mixture, respectively.

In the simulations with $N = 16{,}384$ molecules for heating and cooling experiments, 200 cpp was enough to see the mixture fully cooled or heated. Upper and lower wall temperatures dictated the temperature within the domain. The rate of change of total energy followed the exponential behaviour that is seen in the analytical solutions of the time dependent one dimensional simple energy equation

$$\rho C_{\mathrm{v}} \frac{\partial T}{\partial t} = \kappa \frac{\partial^2 T}{\partial y^2}, \tag{22}$$

where ρ, t and C_{v} represent density, time and specific heat at constant volume, respectively.

Note that, for equal number of helium and argon molecules in the box, one can deduce the following relationships for the estimation of $\langle \rho C_{\mathrm{v}} \rangle$ in Equation (22):

$$\langle \rho C_{\mathrm{v}} \rangle = \frac{N}{2L_x L_y L_z} \langle m C_{\mathrm{v}} \rangle = \frac{3}{4} \frac{kN}{L_x L_y L_z} = \frac{3}{4} \frac{k}{s^3}. \tag{23}$$

According to this formulation, since k is a constant, $\langle \rho C_{\mathrm{v}} \rangle$, a weighted specific heat at constant volume, merely depends on molecular spacing, regardless of molecular mass or diameter.

Defining

$$\varsigma \equiv \frac{\pi^2 \kappa}{\rho C_{\mathrm{v}} L_y^2} = \frac{4\pi^2 s^3 \kappa}{3kL_y^2} = \text{const.} \tag{24}$$

one can solve Equation (22) using the prescribed conditions to get

$$\frac{T(y,t) - T_{\mathrm{w}}}{T_0 - T_w} = \sum_{\xi=1,\,\mathrm{odd}}^{\infty} \frac{4}{\pi\xi} \sin\left(\frac{\xi \pi y}{L_y}\right) \mathrm{e}^{-\xi^2 \varsigma t}, \tag{25}$$

where T_{w} is temperatures on the walls and T_0 is the initial constant temperature in the region. This behaviour is shown in Figure 8.

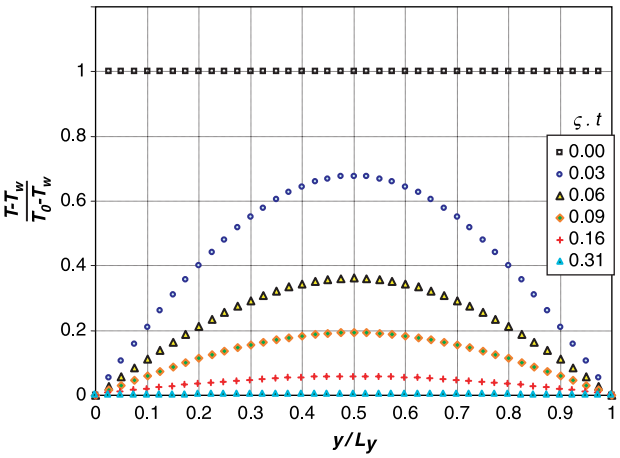

Figure 8. Transient 1D heat conduction, analytical results.

For the sake of qualitative investigation, profiles for heating and cooling simulations are presented herein as in Figure 9. Temperature behaviour of the mixture at 25 cpp qualitatively agrees with the theoretical approach presented in Figure 8. It was also noted that heating/cooling strongly affected argon molecules' number density profiles and helium molecules' energy profiles. Similar behaviour was observed in the simple heat conduction simulations presented in Figure 6.

5. Conclusions

Binary diffusion of helium and argon was examined using a hard-sphere MD simulation method. Binary mass diffusion of gases in two equally sized halves of a box was simulated for same kinetic energies and number densities in low spacing ratio evaluations. After the diffusion process, Maxwellian behaviour was observed for both species. During the diffusion, it was observed that lighter molecules (He) diffused into the heavier ones (Ar) faster. However, energy in the half which initially occupied by He remained, mostly, higher than the other half during the diffusion.

Heat transfer and Couette flow simulations were also conducted. In simple Couette flow runs, two opposite walls were modelled as moving in opposite directions. Modelling heat conduction was accomplished by assigning different fixed average energies to the diffusely reemitted molecules from the two opposite walls. The combined effect of these two wall conditions was examined as well. Energy of heavier molecules is found to be more sensitive to the wall velocities and less sensitive to the wall temperatures than lighter molecules.

Heat conduction, viscosity coefficients and mean free path were also calculated through the MD simulations conducted in cases mentioned above. Results agree with the previous theoretical and simulation studies.

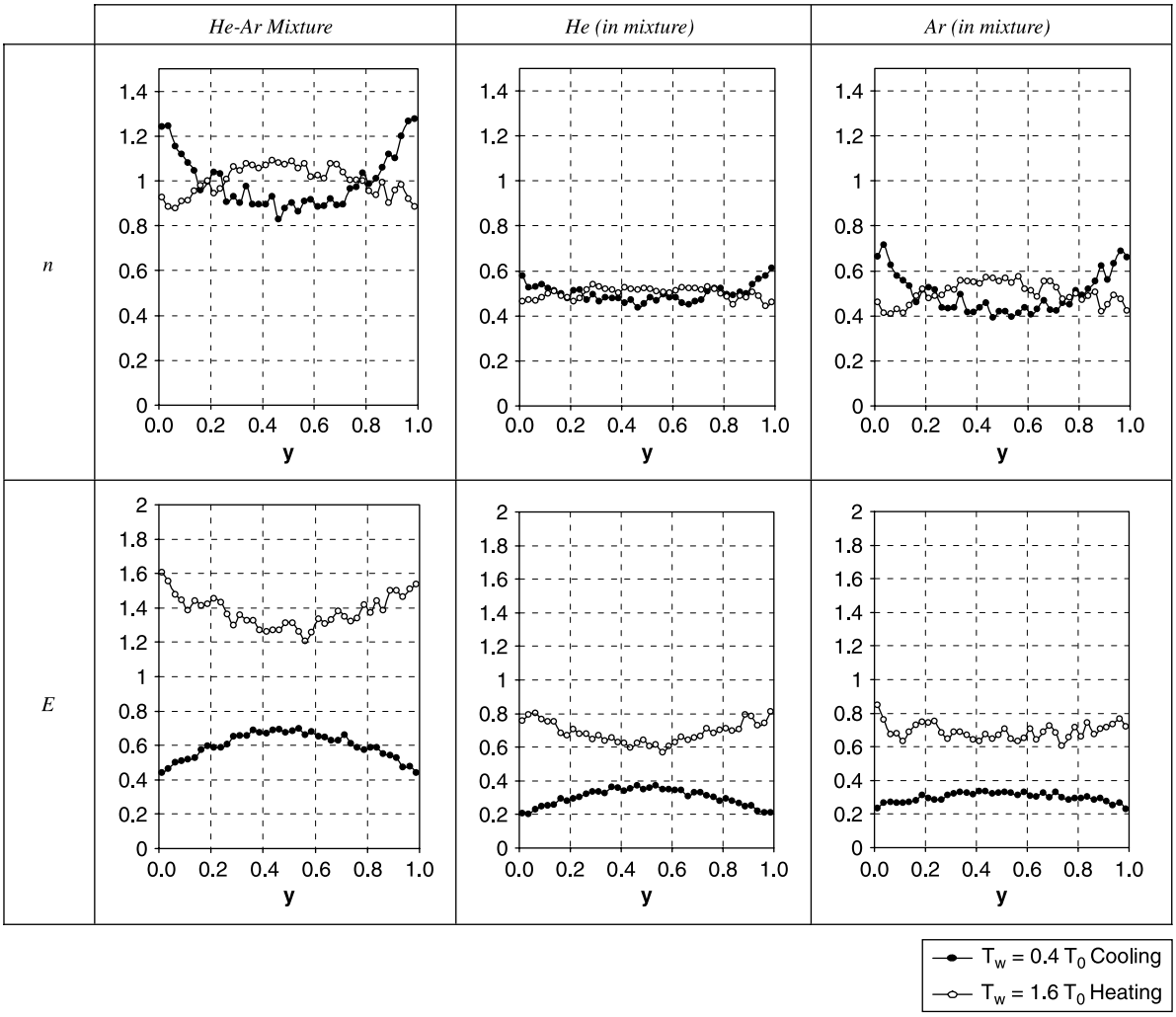

Figure 9. Number density (n) and energy (E) profiles in heating/cooling for the mixture, He only, and Ar only in He–Ar mixture at 25cpp. N = 16384; $s/d_{He} = 5$; Kn ≅ 0.051.

Heating and cooling of the gas mixtures in computational domain were simulated. Heating/cooling strongly affects argon molecules' number density profiles and helium molecules' energy profiles.

As future studies, simulations with different molecules and higher number of molecular species can be examined in order to see whether similar behaviour is observed. Simulations of molecules with higher degrees of freedom are also interesting area to research.

Note

1. Email: sevilgen@bilmuh.gyte.edu.tr

References

[1] J.C. Maxwell, *On the dynamical theory of gases*, Proc. R. Soc. Lond. 15 (1867), pp. 167–171.
[2] M. Knudsen, *The Kinetic Theory of Gases*, McGraw-Hill Book Co. Inc., London, 1946.
[3] J.C. Maxwell, *Scientific Paper*, W.D. Niven, ed., Cambridge University Press, Cambridge, 1890.
[4] L. Boltzmann, *Further studies on the thermal equilibrium of gas molecules*, Sitzungstbenchte Akad. Wiss. Part II Vienna 66 (1872), pp. 275–370.
[5] O.E. Meyer, *Kinetic Theory of Gases*, translated and revised by R.E. Baynes, Longmans, Green and Co., London, 1899.
[6] S. Chapmann, *The kinetic theory of simple and composite monatomic gases: Thermal conduction, and diffusion*, Proc. R. Soc. Lond. A 93 (1916–17), pp. 1–20.
[7] D. Enskog, *Kinetic Theory of Processes in Dilute Gases*, translated by J. Kopp, Almqvist & Wiksells Boktryckeri-A. B., Uppsala, 1917.
[8] S. Chapman and T.G. Cowling, *The Mathematical Theory of Non-Uniform Gases*, 3rd ed., Cambridge University Press, Cambridge, 1970.
[9] A. Rahman, *Correlations in the motion of atoms in liquid argon*, Phys. Rev. 136A (1964), p. 405.
[10] M. Gad-el-Hak, *Liquids: The holy grail of microfluidic modeling*, Phys. Fluids 17 (2005), pp. 100612.1–100612.13.
[11] B.J. Alder and T.E. Wainwright, *Phase transitions for a hard sphere system*, J. Chem. Phys. 27 (1957), pp. 1208–1209.
[12] J.M. Haile, *Molecular Dynamics Simulations*, John Wiley & Sons, Inc., New York, NY, 1992.

[13] I. Kandemir, *A multi-cell molecular dynamics method*, Ph.D. diss., Case Western Reserve University, 1999.
[14] J.L. Barber, K. Kadau, T.C. Germann, P.S. Lomdahl, B.L. Holian, and B.J. Alder, *Atomistic simulation of the Rayleigh–Taylor instability*, J. Phys. Conf. Ser. 46 (2006), pp. 58–62.
[15] H.E. Smorenburg, R.M. Crevecoeur, and I.M. de Schepper, *Fast sound in a dense helium argon gas mixture*, Phys. Lett. A 211 (1996), pp. 118–124.
[16] M. Sampoli, U. Bafile, E. Guarini, and F. Barocchi, *Dynamic structure of He–Ne mixtures by molecular dynamics simulation: From hydrodynamic to fast and slow sound modes*, Phys. Rev. Lett. 88 (2002), p. 085502.
[17] A. Dawid and Z. Gburski, *Interaction-induced absorption in liquid argon–xenon mixture cluster: MD simulation*, J. Mol. Struct. 614 (2002), pp. 177–182.
[18] J. Koplik and J.R. Banavar, *Continuum deductions from molecular hydrodynamics*, Annu. Rev. Fluid Mech. 28 (1995), pp. 257–292.
[19] E. Fermi, G. Ciccotti, and W.G. Hoover (eds.), *Molecular Dynamics Simulation of Statistical–Mechanical Systems*, North-Holland, Amsterdam, 1986.
[20] Y. Zhu, X. Lu, J. Zhou, Y. Wang, and J. Shi, *Prediction of diffusion coefficients for gas, liquid and supercritical fluid: Application to pure real fluids and infinite dilute binary solutions based on the simulation of Lennard-Jones fluid*, Fluid Phase Equilib. 194–197 (2002), pp. 1141–1159.
[21] D. Risso and P. Cordero, *Dilute gas Couette flow: Theory and molecular dynamics simulation*, Phys. Rev. E 56 (1997), pp. 489–498.
[22] I. Kandemir, I. Greber, M. J. Woo, R. Brun, et al. (eds.), *Rarefied Gas Dynamics – Marseille 1998: Heat Conduction and Couette Flow in a Hard Sphere Gas Using a Multicell Molecular Dynamics Computational Method*, Cépaduès Editions, Toulouse, France, 1999.
[23] R.C. Reid, J.M. Prausnitz, and B.E. Poling, *The Properties of Gases and Liquids*, 4th ed., McGraw-Hill, New York, 1987.
[24] G.A. Bird, *Molecular Gas Dynamics*, Clarendon Press, Oxford, 1976.
[25] T. Ohwada, K. Aoki, Y. Sone, and E.P. Muntz (eds.), *"Heat Transfer and Temperature Distribution in a Rarefied Gas Between Two Parallel Plates with Different Temperatures: Numerical Analysis of the Boltzmann Equation for a Hard Sphere Molecule" in Rarefied Gas Dynamics: Theoretical and Computational Techniques*, AIAA, Washington, DC, 1989.